



Synthesis and spectroscopic properties of pyridones – Experimental and theoretical insight



M. Nawaz, S. Hisaindee*, J.P. Graham, M.A. Rauf, N. Saleh

Chemistry Department, PO Box 15551, UAE University, Al-Ain, United Arab Emirates

ARTICLE INFO

Article history:

Received 26 June 2013

Received in revised form 8 December 2013

Accepted 17 December 2013

Available online 29 December 2013

Keywords:

Pyridone

Absorption spectra

NMR

DFT

Tautomerism

Preferential solvation

ABSTRACT

Cyano pyridone (CPy) and its substituted derivatives ($-\text{OCH}_3$ and $-\text{NO}_2$) were synthesized and their absorption spectra were examined in different solvents. The absorption spectra of CPy in different solvents indicated a dependence on the polarizability of the solvent. NMR studies of the keto and enol equilibrium in CPy revealed temperature dependence, with the keto form being more predominant. The equilibrium constant values were in agreement with the theoretical calculations. The calculated pK_a value for CPy was found to be 9.50 ± 0.57 , whereas, for the nitro and methoxy substituted CPy, the values were 8.52 ± 0.36 and 11.04 ± 0.21 respectively. In mixed solvent systems, the preferential solvation was observed in DMSO/ CH_2Cl_2 mixtures, whereas in DMSO/*i*-PrOH, the mixture behaved ideally. The calculations using the PCM model indicated ΔG° values favoring the keto form in both dichloromethane and DMSO. The calculated transition energies were found to be higher than those observed experimentally. For each compound, the keto form was predicted to absorb at a lower energy than the enol form. The main transition of both forms of CPy corresponded to a $\pi-\pi^*$ transition from the HOMO \rightarrow LUMO of the compound.

© 2013 Elsevier B.V. All rights reserved.

1. Introduction

The electronic absorption spectra of various molecules are effected by solvents and form the basis of scientific studies of photophysics of the excited states [1–6]. The spectral data can be used to extract important information especially when the solute molecules can absorb and emit radiation translated in the form of electronic spectra. In solutions, the environment of the solvent largely determines the changes in the electro-optical properties of the probe molecule as compared to those in its gaseous phase. The spectral behavior of the solute molecule largely depends on the strength of the intermolecular forces (such as hydrogen bond) between the substituent groups of the solute molecule and the surrounding solvent molecules. The solvent polarity also plays an important part in determining the spectral position of the molecular systems which do not form intramolecular bond. Several reports are now available on the correlation of absorption spectra with the solvent parameters [7–11].

In many cases mixed solvent systems have also been used to study solvent–solute interactions [12,13]. In solvent mixtures, the solute microenvironment may be different in comparison to the bulk solvent composition due to the difference between the nature and extent of interaction of the solute with component solvents. Herein, the interaction occurs when the polar solute has in its microenvironment more

of one solvent than the other in comparison to the bulk composition. This phenomenon is termed as preferential solvation and the interactions in mixed solvents are more complex as compared to that of pure solvents. Physicochemical properties of the solute, solvents, and the micro-heterogeneity in the solvent mixture would affect the preferential solvation. The data can be used to interpret the kinetic, spectroscopic and equilibrium behavior in mixed solvents which are important to understand various physico-organic reactions of many organic molecules. Molecules capable of undergoing acid–base equilibria are affected by the solvent types and are sensitive to pH changes [14].

Chemical compounds such as phenols, pyridines and pyridones undergo intramolecular proton transfer, a process called as tautomerism. The energy differences between the structurally different tautomers are usually as small as a few kcal/mol. Thus a thorough study of the relative stability of close-lying tautomers typically requires the use of computational techniques to supplement the experimental findings. Cyano-pyridones (CPy) are an important class of compounds which have shown antipathogenic properties and are of scientific interest [15,16]. They can undergo acid–base equilibrium, and thus it would be of interest to look at the effect of various solvents on these molecules and explain the behavior in terms of solvent properties. The keto–enol tautomerism of the parent pyridone has been studied, however, not much work has been reported on the solvatochromic behavior of this compound [17]. In this paper, CPy with various substituents ($-\text{OCH}_3$ and $-\text{NO}_2$) in different solvents were studied in order to understand the effect of specific and non-specific interactions on solvation of these molecules.

* Corresponding author. Tel.: +971 3 7136140; fax: +971 3 7134928.

E-mail address: soleiman.hisaindee@uaeu.ac.ae (S. Hisaindee).

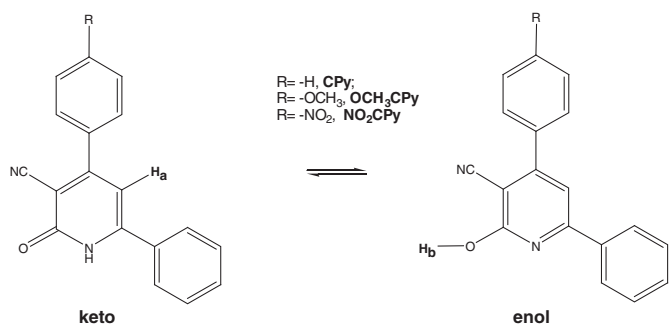


Fig. 1. Tautomeric forms of cyanopyridones.

2. Experimental

All reagents and materials were purchased from Sigma-Aldrich and used without further purification. Thin-layer chromatography (TLC) was performed on silica gel glass plates (Silica gel, 60 F₂₅₄, Fluka) and spots were visualized under UV lamp. Melting points were obtained on a Gallenkamp apparatus and are uncorrected. Infrared spectra were measured using KBr pellets on a Thermo Nicolet model 470 FT-IR spectrophotometer. ¹H-NMR and ¹³C-NMR spectra were recorded on Varian NMR instrument at 400 MHz and 100 MHz respectively in DMSO-*d*₆ solutions using tetramethylsilane (TMS) as an internal reference.

2.1. Synthesis of pyridones, their derivatives and characterization

A mixture of acetophenone (366 mg, 3.0 mmol), benzaldehyde, anisaldehyde or nitroaldehyde (3.0 mmol), ethyl cyano-acetate (339 mg, 3.0 mmol) and ammonium acetate (1.85 g, 24 mmol) was heated, with stirring, in a microwave reactor at 110 °C (dynamic power 50–60 W) for 25 min. The resulting solid was washed with cold water, recrystallized from hot ethanol and dried under vacuum.

Cyanopyridone: yellow solid (620 mg, 76%); m.p. > 300 °C (decomposed), IR (KBr, cm⁻¹): 3135, 3022, 2898, 2217, 1646, ¹H NMR (400 MHz, DMSO-*d*₆) δ (ppm) (mixture of tautomers) 6.79 (s br, 0.9H), 7.48–7.70 (m, 6H), 7.69–7.70 (m, 2H), 7.86–7.88 (m, 2H), 12.81 (s br, 0.3 H); ¹³C NMR (100 MHz, DMSO-*d*₆) δ (ppm) (mixture of tautomers) 99.5 (br), 103.0 (br), 116.9, 128.2, 128.7, 129.2, 129.4, 130.9, 131.7, 136.5, 151.0 (br), 160.5 (br), 162.1 (br).

Methoxyppyridone: light yellow solid (209 mg, 23%); m.p > 300 °C (decomposed); IR (KBr, cm⁻¹): 3444, 3033, 2934, 2220, 1651; ¹H NMR (400 MHz, DMSO-*d*₆) δ (ppm) (mixture of tautomers) 3.30(s, 3H), 6.75(s br, 1H), 7.03–7.11 (m, 2H), 7.48–7.54(m, 3H), 7.69–7.72(m, 2H), 7.84–7.86(m,2H), 12.81 (s br, 0.4H); ¹³C NMR (100 MHz, DMSO-*d*₆) δ (ppm) (mixture of tautomers) 55.89, 99.2 (br), 106.3 (br), 114.67, 117.29, 128.17, 128.45, 129.35, 130.49, 131.56, 151.0 (br), 160.0 (br), 161.58, 162.3 (br).

Nitropyridone: Light orange solid (420 mg, 44%); m.p > 300 °C (decomposed), IR (KBr, cm⁻¹): 3448, 3063, 2948, 2217, 1654; ¹H NMR (400 MHz, DMSO-*d*₆) δ (ppm) (mixture of tautomers) 6.89 (s br, 0.8H), 7.48–7.57 (m,4H), 7.88–7.99 (m, 4H),8.36–8.39 (m, 2H),12.91 (s br, 0.3H); ¹³C NMR (100 MHz, DMSO-*d*₆) δ (ppm) (mixture of tautomers) 109.0, 113.8, 116.4, 118.0, 124.3, 128.0, 128.3, 129.3,129.4, 130.4, 131.8, 142.7, 148.9.

2.2. Sample preparation and UV studies

Although the range of solvents was limited by the solubility of the compounds, it was suitable enough to estimate the role of solvent

polarity, polarizability, and hydrogen bond donating power. The solvents used in this work were, Water, DMSO, DMF, Dichloromethane, Ethylene glycol, Acetone, Isopropanol, Toluene, Methanol, THF and Acetonitrile, all of which were purchased from Merck or Fluka and had a purity of >99%. They were kept over molecular sieves 4 Å for at least 3 days prior to their use in this work. Stock solutions of the compounds were made in all these solvents and further dilutions were done with a given solvent. Absorption spectra of each solution was recorded on a CARY 50 UV/vis spectrophotometer, using a 1 cm quartz cell. Binary mixtures of isopropanol + DMSO and DMSO + dichloromethane were prepared by weighing the solutions in a quartz cuvette (the co-solvent solution was added with a 1 mL microsyringe) and the final values were expressed in terms of the co-solvent mole fraction (*X*₂) in the mixtures. All experiments with the mixed solvent systems were carried out at room temperature (23 ± 2 °C) in duplicate.

2.3. NMR studies

The temperature dependence of the equilibrium between the keto and enol tautomers was studied using a Varian 400 MHz NMR instrument. Spectra of a sample of Cyano pyridone (CPy) (10 mg/0.6 mL DMSO-*d*₆) were recorded at temperatures ranging from 25 to 65 °C with a 5 °C increment. The keto/enol ratios were then calculated from the peak integration of a non-exchangeable C–H peak at ~6.8 ppm (H_a, Fig. 6) and the enol–OH at ~12.5 ppm (H_b, Fig. 6).

2.4. Computational details

All calculations were performed using Gaussian 09 W rev. C01 [18]. The structure of keto and enol tautomers for each species was optimized using the B3LYP hybrid functional and 6-311 + G(d,p) basis set. Vibrational frequency calculations were performed at the B3LYP/6-311 + G(d,p) level to confirm energy minima and determine free energies for each structure. Electronic spectra were simulated using time-dependent DFT calculations with the CAM-B3LYP functional [19] and 6-311 + G(d,p) basis set. All geometry optimization and electronic spectrum calculations were performed in the gas phase. Additional vibrational frequency calculations were performed using the PCM model [20,21] to simulate solvent effects on the calculated free energies for the solvents DMSO and CH₂Cl₂.

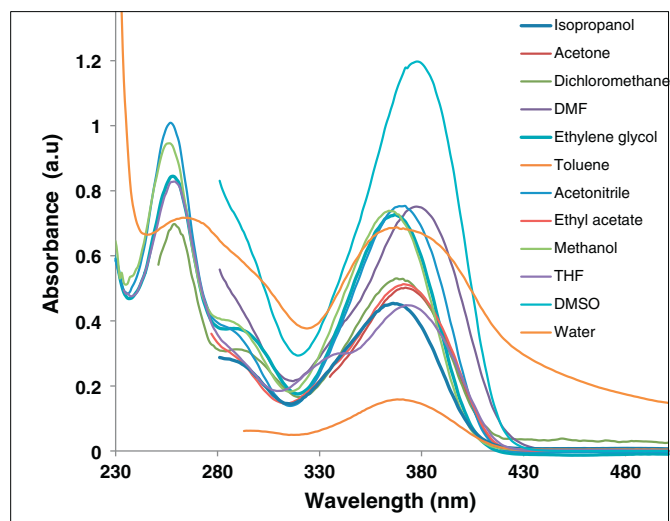


Fig. 2. Absorption spectra of CPy in various solvents.

Table 1
Spectroscopic data of CPy in various solvents and solvent parameters.

Solvent	λ_{\max} (nm)	$\bar{\nu}$ (cm^{-1})	E_T (kcal/mol)	n	f	π^*	ϵ	$f(e,n)$	Donor number (kcal/mol)	Acceptor number
Water	368	27,174	77.7	1.3330	0.304212	1.09	80.1	0.33425	18	54.8
DMSO	378	26,455	75.6	1.4790	0.351847	1.0	47.2	0.30648	29.8	19.3
DMF	377	26,525	75.8	1.4305	0.338327	0.88	36.7	0.30534	26.6	16
Dichloromethane	368	27,174	77.6	1.4241	0.336394	0.82	8.93	0.21578	1	20.4
Ethylene glycol	366	27,322	78.1	1.4318	0.338715	0.92	38.7	0.30692	20	–
Acetone	372	26,881	76.8	1.3587	0.314274	0.71	20.7	0.28929	17	12.5
Isopropanol	366	27,322	78.1	1.3772	0.321004	0.48	18	0.27909	21.1	33.8
Toluene	368	27,174	77.6	1.4969	0.35638	0.54	2.38	0.01057	0.1	0.11
Methanol	364	27,472	78.5	1.3280	0.30215	0.60	33	0.31302	19	41.5
THF	372	26,881	76.8	1.4070	0.331041	0.58	7.52	0.19997	20	8
Acetonitrile	372	26,881	76.8	1.3440	0.308625	0.75	38.8	0.31691	14.1	16.9
Ethyl acetate	371	26,954	77.1	1.3724	0.319296	0.55	6.02	0.17901	17.1	9.3

2.5. Results and discussion

When absorption spectra are recorded in solvents of different polarity, it is found that the positions, intensities and shapes of the absorption bands are usually modified. Usually, the spectral shifts are attributed to specific solute–solute and solute–solvent interaction in the form of hydrogen bonding and/or bulk solvent properties. Apart from these interactions, there are several other factors that may influence the spectra such as acid–base chemistry or charge transfer interactions [22]. Solvatochromic effect has been used to determine the magnitude of the solute–solvent interactions such as the polarizability/dipolarity parameter, π^* , of the solvent, as well as giving information about hydrogen bond donor (HBD), α and/or hydrogen bond acceptor (HBA), β ability of the solvent. In many molecules, the bands ($n-\pi^*$, $\pi-\pi^*$) are shifted bathochromically when the solvent polarity increases. These changes are attributed to hydrogen-bonding interaction between the solute and the solvent molecule. On the other hand, the spectral shifts in the molecular systems with intramolecular hydrogen bonds are very small. In purely intramolecular hydrogen bonded systems, the solvent shifts have been interpreted by the solvent polarity function [23].

The molecular structure of CPy, as shown in Fig. 1, can exist in both the keto and enol forms. The equilibrium between the two species can be easily probed by using UV and NMR techniques. However, if the energy barrier between the two tautomeric species is small, and have overlapping spectra, UV technique cannot be used to study the equilibria. In that case, NMR studies would be more informative. The equilibrium is also affected by the substituents and thus in our present study, we compared the spectral behavior of parent CPy with substituted derivatives containing either an electron donating group ($-\text{OCH}_3$) or an electron withdrawing group ($-\text{NO}_2$).

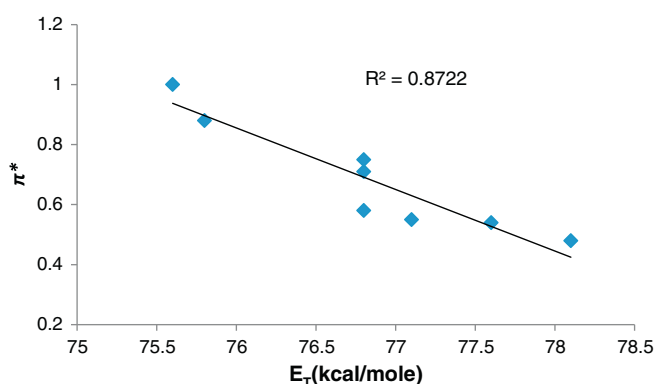


Fig. 3. Change in E_T values as a function of solvent polarizability (π^*).

2.6. Solvent effect on absorption spectra

The absorption peak of CPy appears as a single band in all the solvents as shown in Fig. 2. The change in peak position of the absorption band in different solvents is an indication that the absorption wavelengths are affected by the nature of the solvent. For example, with an increase of solvent polarity, the λ_{\max} of the probe molecule was red-shifted by 14 nm (from 364 nm in methanol to 378 nm in DMSO). The shift to longer wavelength could be due to either the destabilization of the highest occupied molecular orbital (HOMO) or the stabilization of the lowest unoccupied molecular orbital (LUMO). Observed red-shifts in the absorption wavelengths suggest that these solvents stabilize the excited state of the probe molecule to various extent. The shift in spectral position can thus be targeted to investigate the solute–solvent interaction of the molecule in various solvents.

The absorption data of CPy in various solvents were firstly analyzed in terms of polarity scale. The method involves the transformation of λ_{\max} (nm) of the compound in various solvents into molar transition energies by using the following relationship [24]:

$$E_T \left(\text{kcal mol}^{-1} \right) = 28591 / \lambda_{\max} \text{ (nm)} \quad (1)$$

The E_T values signify transition energy which also reflects the stabilization of the molecule in its ground state in a given solvent. This may be due to either hydrogen bond formation or solute–solvent interaction. Thus, E_T provides a direct empirical measure of molecule's solvation behavior. From Table 1, one can see that E_T is maximum in the case of methanol as compared to other solvents, which reflects the strong association of the probe molecule with methanol. The graphical trend of E_T values versus π^* (dipolarity/polarizability) is shown in Fig. 3.

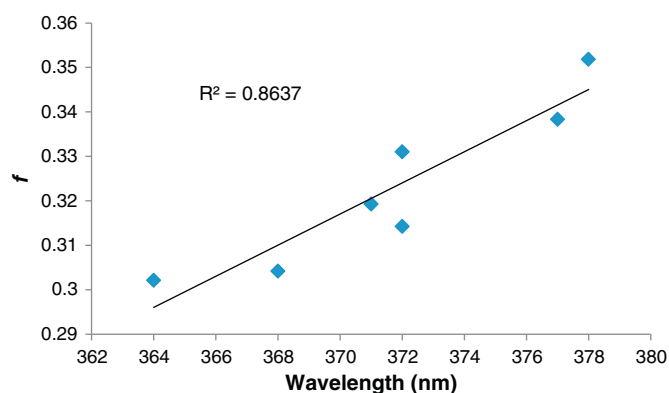


Fig. 4. Plot of polarization red shift versus f value in various solvents.

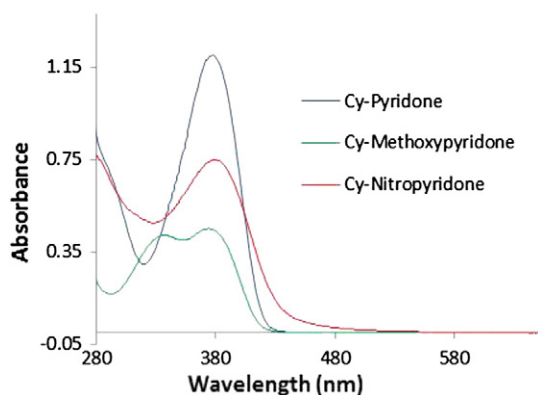


Fig. 5. Absorption spectra of CPy and its derivatives.

Close inspection of Table 1 shows a similar correlation between π^* , donor (DN) and acceptor numbers (AN) and molar transition energy (E_T). As π^* , DN and AN values decrease, E_T value increases, which shows that CPy has an equal ability to act as a donor and acceptor species.

The electronic absorption spectra of CPy in the various solvents were secondly analyzed by plotting $f = (n^2 - 1) / (2n^2 + 1)$, (where n is the refractive index of the solvent), versus the λ_{max} (nm) of the probe molecule in various solvents as shown in Fig. 4. The linear nature of the plot ($R^2 = 0.8637$) suggests that the red shifts in the absorption band are mainly a result of solvation rather than coordination. Behavior of the investigated substituted CPy is expected to be similar to that of their un-substituted counterpart. However, the absorption spectra of the methoxy substituted cyano pyridine shows two prominent absorption peaks (Fig. 5) which can be attributed to two different electronic transition states. A detailed study in this regard is under investigation.

2.7. NMR studies

NMR studies of the parent compound (unsubstituted CPy) were performed in deuterated DMSO- d_6 and $CDCl_3$ solutions to establish the keto–enol tautomerism in the CPy molecule. The results are shown in Fig. 6. It can be seen from this figure that the probe molecule can exist in solution (DMSO, $\mu = 3.96$ D) in both keto and enol forms. The peak at ~ 12.5 ppm is attributed to the enol hydroxyl group (H_b in Fig. 1) which was easily exchanged when the sample was shaken with D_2O . The peak at ~ 6.8 ppm is ascribed to the non-exchangeable proton H_a of the keto form. On the other hand, the NMR spectra in $CDCl_3$ revealed

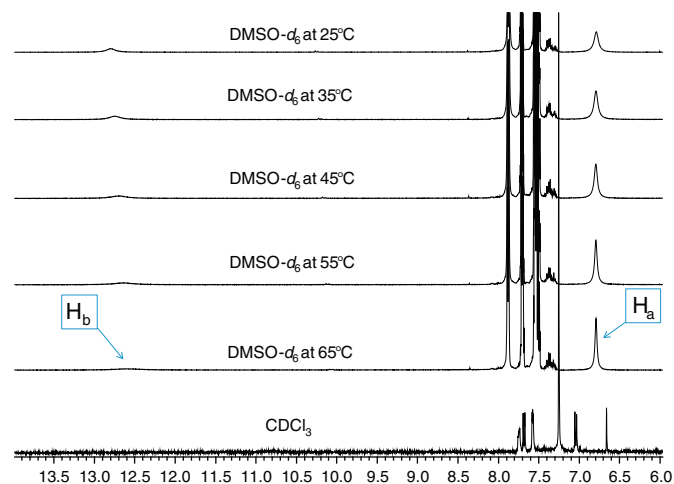


Fig. 6. 1H NMR spectra CPy in $CDCl_3$ and DMSO- d_6 at different temperatures.

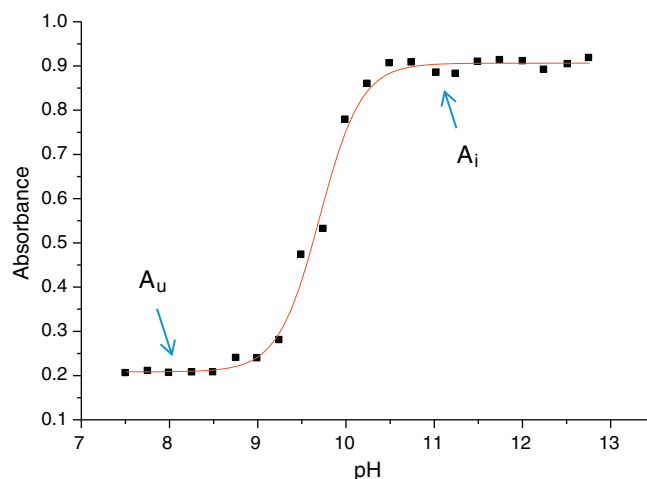


Fig. 7. Change in absorption value of CPy at various pH.

that the keto form is the only species present at room temperature. From the observed NMR study, it can be inferred that the keto form is more stabilized in a less polar environment ($CDCl_3$, $\mu = 1.04$ D).

The effect of temperature on keto–enol tautomerism was also investigated by changing the temperature of DMSO- d_6 solution of CPy. An increase in temperature of the solution causes an increase in the NMR signal attributed to keto form (H_a) with a simultaneous decrease in enol peak (H_b). Also there is a flattening and slight upfield shift in H_b signal as temperature is increased. On the other hand, the H_b signal did not shift with temperature increase but became sharper. Thus one can infer that the keto–enol tautomeric equilibria for the probe molecule is sensitive to temperature changes. The ratio of the integration H_a/H_b is an indication of the equilibrium constant of the two tautomers (keto \rightarrow enol) at a given temperature. Thus the spectra of CPy in DMSO- d_6 were recorded at temperatures ranging from 25 to 65 $^{\circ}C$ with 5 $^{\circ}C$ increment. K_{eqib} was calculated from the NMR data using the peak ratios of keto and enol forms at different temperatures. A plot of $1/T$ vs. $\ln K_{eqib}$ was used to calculate ΔG according to the following equation:

$$\Delta G = -RT \ln K_{eqib}. \quad (2)$$

The calculated value of ΔG for CPy was found to be 5.14 kJ/mol, whereas, for the nitro and methoxy substituted CPy, the values were 2.16 kJ/mol and 2.51 kJ/mol respectively. Thus one can infer that the presence of substituents causes a change in the ΔG value. The experimental ΔG values are close to the theoretical values as per DFT calculations shown in the later part of this paper.

2.8. Effect of solution pH

Although the absorbance spectra of CPy were observed to change in a wide variety of solvents, the absorbance spectra was also found to be sensitive to the pH of the aqueous solutions. Absorption spectra of CPy in 15% DMSO aqueous solution at different pH values were monitored to determine the acid dissociation constants (K_a) of the molecules under investigation. An S-shaped curve was obtained when the absorbance values were plotted against the pH of solution (Fig. 7). From this curve one can determine the dissociation constant using the following relationship [24]:

$$pK_a = pH + \log [(A_i - A)/(A - A_u)] \quad (3)$$

In the above equation, the value A relates to the absorbance of the parent CPy molecule at a particular pH and wavelength. pK_a values were computed at different wavelengths in the range 359–369 nm and at pH values of 9.25 and 10.25. The values of A_u and A_i were obtained

Table 2Calculated pK_a values for CPy at different pH and wavelength.

pH	Selected wavelength (nm)						
	359	361	363	365	367	369	
9.25	10.21524	10.21628	10.23474	10.23759	10.21288	10.26383	
9.5	9.75219	9.755359	9.753139	9.758249	9.503053	9.51581	
9.75	9.826043	9.831384	9.830404	9.832912	9.328036	9.337321	
10	9.366161	9.376975	9.357346	9.383985	8.619137	8.623549	
10.25	9.147903	9.148255	9.10676	9.144513	8.158764	8.159938	
$pK_a = 9.50 \pm 0.57$							

from pH vs. absorbance plots for each wavelength used in the calculation. The calculated value of pK_a for CPy as shown in Table 2 was found to be 9.50 ± 0.57 , whereas, for the nitro and methoxy substituted CPy, the values were 8.52 ± 0.36 and 11.04 ± 0.21 respectively. Thus one can infer that the presence of an electron withdrawing group ($-\text{NO}_2$) cause the pK_a to decrease and the electron donating group ($-\text{OCH}_3$) causes the pK_a to increase.

2.9. Spectra in binary solvent mixtures

Studies concerning the interaction of solutes in mixed solvents have been reported in the literature [25–27]. Solutes behave in a different way in mixed solvent systems and their behavior is more complex than in pure solvents due to preferential solvation, which occurs when the solute has a selective environment of one solvent than the other in a mixture. In a binary mixture, one component of the mixture preferentially interacts with the molecule in its vicinity to form additional intermolecular interactions such as hydrogen bonding or dipole–dipole interactions.

To understand the solute–solvent interaction of CPy in mixed solvents, the UV–vis spectra of the molecule were recorded in mixtures of DMSO + dichloromethane (CH_2Cl_2) and DMSO + iso-propanol (*i*-PrOH) mixtures in various proportions. Dimethyl sulfoxide (DMSO) is an aprotic polar solvent with a dipole moment (μ) of 3.96 D and dielectric constant (ϵ) of 47.24. On the other hand, CH_2Cl_2 is also aprotic polar solvent which has a μ value of 1.55 D and $\epsilon = 8.93$, whereas, *i*-PrOH is a polar protic solvent with $\mu = 1.56$ and $\epsilon = 18$. In these conditions, a mixture of DMSO with either CH_2Cl_2 or *i*-PrOH should provide an interesting combination to study the solvent dependence changes on the absorption spectra of the probe molecule.

If the mixture of solvents behaves ideally, then the solvent–solvent interactions are negligible and the transition energy (calculated from absorbance spectral data), $\bar{\nu}_{12}$, is given by the relationship:

$$\bar{\nu}_{id} = X_1\bar{\nu}_1 + X_2\bar{\nu}_2 \quad (4)$$

where $\bar{\nu}_1$, $\bar{\nu}_2$ and $\bar{\nu}_{id}$ are the wavenumbers of the absorption maximum in solvent 1 and solvent 2, and their ideal binary solvent mixtures respectively, X_1 and X_2 represent the mole fractions of the two solvents. For the ideal solvation in a binary solvent mixture, a plot of $\bar{\nu}_{id}$ as a function of mole fraction of the solvents should be linear over the entire range of mole fractions. Any deviation from the linearity of this plot is an indication that the solute is preferentially solvated by one of solvents [28]. The observed $\bar{\nu}_{mix}$ of a probe molecule in binary solvent mixtures depends on the composition of the solvent mixture. Under these conditions $\bar{\nu}_{mix}$ can be related to the cybotactic composition by the equation:

$$\bar{\nu}_{mix} = \bar{\nu}_1 X_1^L + \bar{\nu}_2 X_2^L \quad (5)$$

where X_1^L and X_2^L are the mole fraction of solvent 1 and solvent 2 in the cybotactic region of sample. The value of X_1^L is generally different from that of X_1 because of solute–solvent interactions and solvent–solvent interactions. The mole fraction X_2^L of the solvent 2 can be estimated by using the following equation:

$$X_2^L = (\bar{\nu}_{mix} - \bar{\nu}_1) / (\bar{\nu}_2 - \bar{\nu}_1) \quad (6)$$

The degree of deviation from the ideality can be expressed by the excess function, δs_2 , defined as the difference between X_2^L and X_2 . For values of $\delta s_2 > 0$ the solute is preferentially solvated by solvent 2, whereas, when $\delta s_2 < 0$ a preference for solvent 1 is given over solvent 2.

The preferential solvation of the solute in binary mixed solvents can be analyzed by using the preferential solvation constant (K_{PS}) as reported in the literature [29].

$$K_{PS} = (X_1^L / X_2^L) / (X_1 / X_2) \quad (7)$$

Preferential solvation constant measures the tendency of a given sample to be solvated by solvent 1 as compared to solvent 2. When $K_{PS} > 1$, solvent 1 (CH_2Cl_2 or *i*-PrOH) is preferred over solvent 2

Table 3

Parameters related to solvation studies of CPy in solvent mixtures.

Mole fraction DMSO	CH_2Cl_2 + DMSO					Mole fraction DMSO	<i>i</i> -PrOH + DMSO				
	X_2^L	$\bar{\nu}_{12}$ (cm^{-1})	$\bar{\nu}_{12}(\text{id})$ (cm^{-1})	K_{PS}	δs_2		X_2^L	$\bar{\nu}_{12}$ (cm^{-1})	$\bar{\nu}_{12}(\text{id})$ (cm^{-1})	K_{PS}	δs_2
0.1291	0.1496	26,506	26,525	38.32	0.020	0.1102	0.1706	26,174	26,246	0.53	0.060
0.2287	0.1496	26,599	26,525	19.16	−0.079	0.1985	0.2854	26,280	26,385	0.62	0.0868
0.3079	0.2249	26,673	26,595	7.74	−0.059	0.3312	0.4014	26,525	26,440	0.74	0.0702
0.4257	0.3006	26,783	26,666	3.13	−0.125	0.4052	0.4599	26,530	26,596	0.79	0.0547
0.5093	0.4532	26,862	26,809	1.16	−0.056	0.5173	0.5188	26,665	26,667	0.99	0.0015
0.6026	0.5301	26,949	26,881	0.58	−0.007	0.6656	0.6373	26,844	26,810	1.13	−0.028
0.7044	0.4532	27,045	26,809	0.51	−0.251	0.7359	0.6971	26,929	26,882	1.21	−0.038
0.8066	0.6074	27,140	26,954	0.15	−0.199	0.7769	0.6971	26,978	26,882	1.51	−0.008
0.9434	0.8419	27,269	27,173	0.011	−0.101	0.9330	0.8590	27,167	27,174	1.60	−0.074

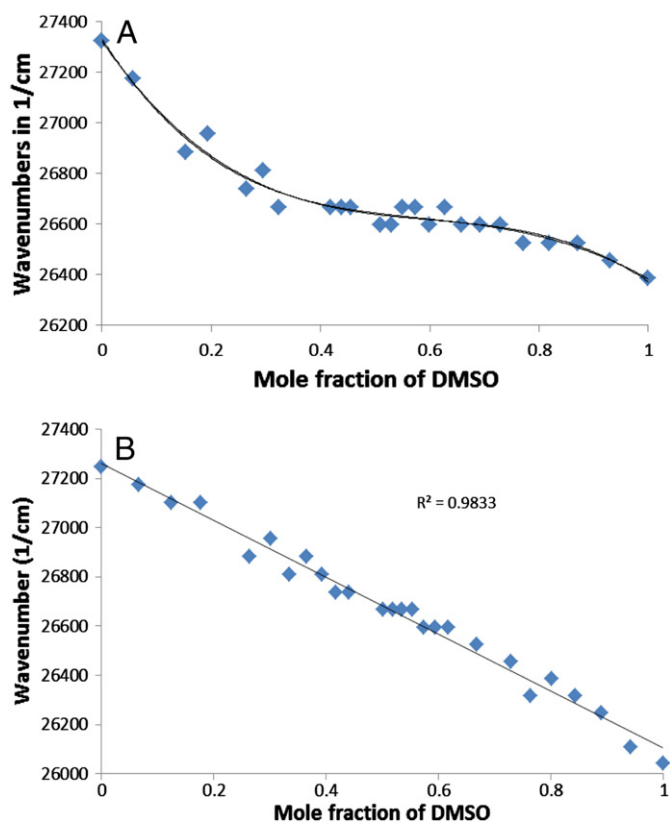


Fig. 8. A. Absorption trend of CPy in CH_2Cl_2 + DMSO. B. Absorption trend of CPy in *i*-PrOH + DMSO.

(DMSO) and for $K_{\text{PS}} < 1$, the opposite is true [30]. Table 3 summarizes the parameters related to solvation studies in mixtures.

In pure CH_2Cl_2 , the probe molecule exhibits an absorption value at 27174 cm^{-1} . On addition of incremental amounts of DMSO, the absorbance peak shifted to lower wavenumbers, which is an indication of positive solvatochromism. The absorbance almost flattens out at ~30 mol% of DMSO in the mixture as shown in Fig. 8A. This suggests that at this concentration, all the probe molecules are now completely solvated by the DMSO, which is due to the highly polar nature of this solvent to engage the organic moiety in forming hydrogen bonded complexes in solution [31]. Incremental increase in the amount of DMSO beyond 0.8 mol fraction causes the spectra to shift the absorption spectra towards the region observed in pure DMSO. The formation of aggregates of the organic moiety in DMSO rich region in CH_2Cl_2 – DMSO mixtures is unlikely as no new additional shoulder peak was observed in the absorption spectra of either the mixture or neat DMSO.

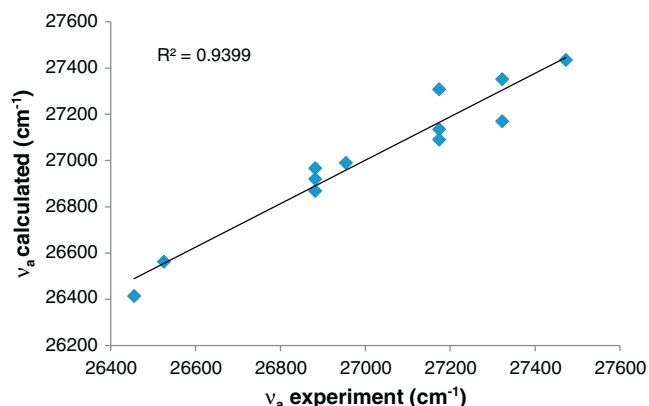


Fig. 9. A fit of the absorption energies to the Kamlet–Abboud–Taft relationship.

A similar experiment was performed using polar protic solvent (*i*-PrOH) and DMSO. A linear change in the absorption wavenumber against DMSO mole fraction was observed. Since both *i*-PrOH and DMSO are polar solvents and capable of making hydrogen bonds with the solute molecule, the microenvironment surrounding the CPy molecule (also a polar molecule) is crowded by the two solvents resulting in a network of hydrogen bonding with the two solvents at the same time. In these mixtures, the interaction between the solvents and the probe molecule can be assumed to be of equal extent. The change in mole fraction of DMSO in the mixture causes the enrichment of the microenvironment by DMSO molecules resulting in the replacement of *i*-PrOH molecules in the solvation shell of CPy molecule by DMSO. This change in the microenvironment does not affect the nature of the probe–solvent mixture interaction. This behavior reflects in the form of linearity ($R^2 = 0.9833$), when $\bar{\nu}$ was plotted against mole fraction of DMSO (Fig. 8B). This was further supplemented from the fact that a linear relationship ($R^2 = 0.9602$) was observed when K_{PS} was plotted against the mole fraction of DMSO.

2.10. Application of Kamlet–Abboud–Taft model

The analysis of solvent effect on spectral properties of CPy solutions was also carried out by using the spectral shift in various solvents and correlating these with the solvatochromic parameters namely, π^* (polarity–polarizability parameter), α (the solvents hydrogen bond donor ability), β (the solvents hydrogen bond acceptance ability), obtained from the literature [32]. The effect of solvent on the absorption energy may be described by the Kamlet–Abboud–Taft model [24]. The Kamlet–Taft equation combines spectroscopic polarity scales including hydrogen bonding donor ability (α), hydrogen bonding accepting ability (β) and dipolarity/polarizability (π^*) as a multiparameter scale. This model has been successfully used to describe solvent effects on spectral properties in the literature and is given by the following relationship.

$$\bar{\nu}_a = \bar{\nu}_0 + s\pi^* + a\alpha + b\beta \quad (8)$$

where $\bar{\nu}$ is the solvatochromic property of interest (in this case absorption energy in cm^{-1}), and the regression coefficients a , b and s in these equations measure the relative susceptibilities of the solute property to the indicated solvent parameters. Multivariate regression was used to fit the absorption energies to the Kamlet–Abboud–Taft relationship, resulting in the following equation:

$$\bar{\nu}_a = 27723 - 1006\pi^* + 645a - 397\beta \quad (9)$$

The negative sign of s and b coefficients indicate a bathochromic shift with both increasing solvent dipolarity/polarizability and solvent hydrogen bond acceptor basicity. This suggests stabilization of the electronically excited state relative to the ground state. The positive sign of a coefficient indicates a hypsochromic shift with increasing hydrogen-bond donor acidity of the solvent. This suggests stabilization of the ground state relative to the electronically excited state. Fig. 9 shows a plot of absorption wavelength versus the predicted absorption wavelength using Eq. (8). The data fits very well to the above model with a R^2 value of 0.9399.

2.11. Theoretical calculations

The structures of keto and enol tautomers of the three compounds were optimized in the gas phase using the B3LYP functional and 6-311 + G(d,p) basis set. Optimized structures along with bond lengths for each species are given in Fig. 10.

2.11.1. Keto–enol tautomerism

Free energies calculated for the keto and enol forms of the three compounds indicate that the keto-form is favored in all cases in the

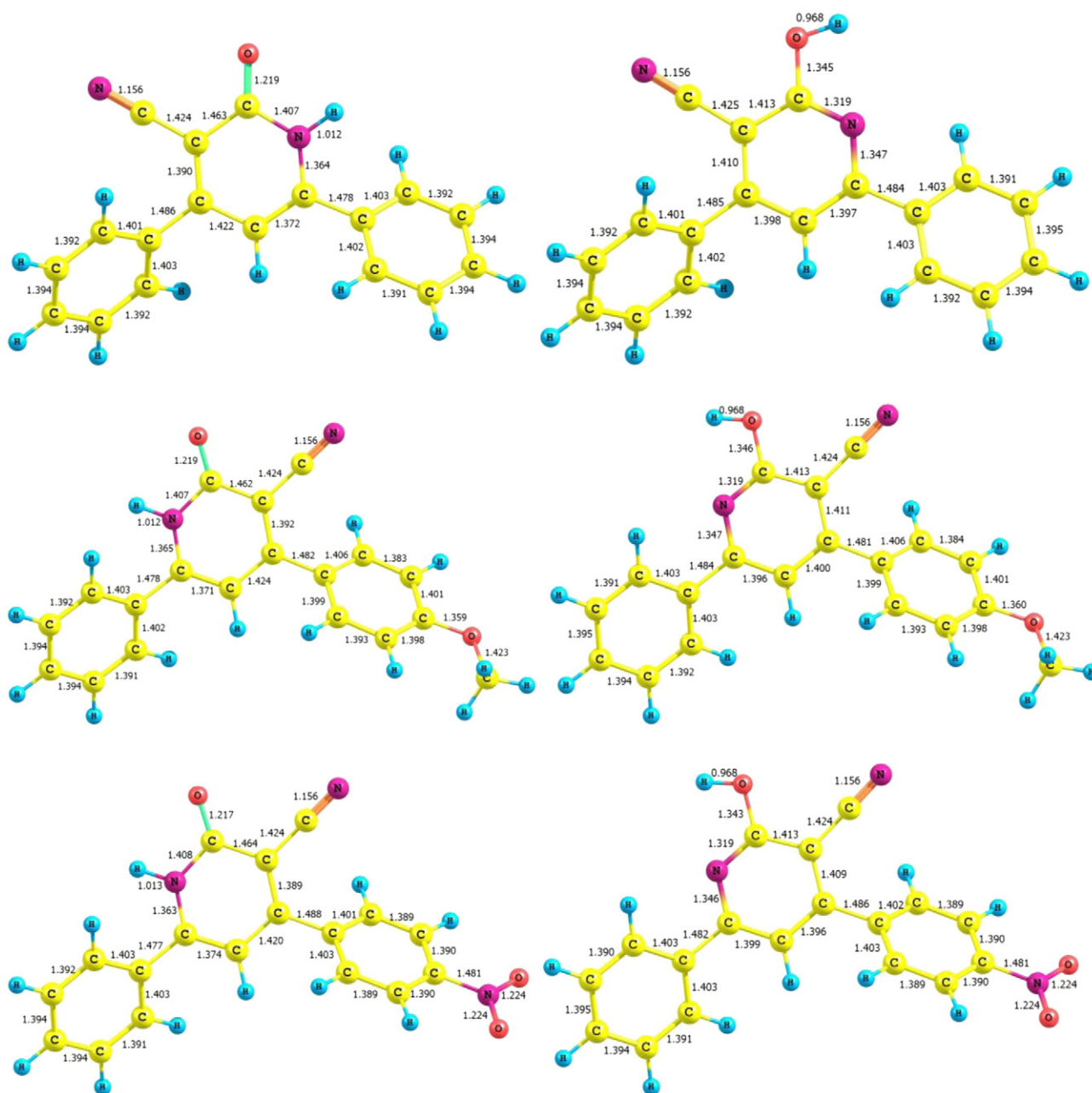


Fig. 10. Optimized structures of tautomers, from top to bottom, CPy, $-OCH_3$ -CPy and $-NO_2$ -CPy; (keto is shown on the left and enol is shown on the right).

gas phase (Table 4). The calculated energy differences between keto and enol tautomers range from 2.4–3.2 kJ/mol. The small difference in free energies is consistent with both tautomers existing in equilibrium with the keto-form being the major form. Given the small free energy differences, it would be reasonable for this equilibrium to be sensitive to solvent effects. The PCM model was used to investigate solvent effects on the equilibrium between keto and enol tautomers of CPy. The calculations using the PCM model indicate ΔG° values favoring the keto form

in both dichloromethane and DMSO (Table 5). Consistent with the experimental data, the preference for the keto form is calculated as greater in DMSO than CH_2Cl_2 . However, the magnitude of ΔG° in both solvents would suggest very little enol-form in either. The ΔG° values for the gas phase are more consistent with the observation of both keto- and enol- forms in CH_2Cl_2 and the experimentally determined values of ΔG° from NMR. Hence it appears that the PCM model exaggerates the difference in solvation energies between the two tautomers.

Table 4

Calculated gas-phase free energies for compounds 1–3 in keto and enol forms.

	CPy		$-OCH_3$ CPy	$-NO_2$ CPy		
Compound	1-keto	1-enol	2-keto	2-enol	3-keto	3-enol
G° (Hartrees)	–877.8958	–877.8948	–992.4240	–992.4228	–1082.4589	–1082.4580
ΔG° (kJ/mole)	2.6		3.2		2.4	

Table 5
Calculated free energies for keto and enol forms of CPy using the PCM model of solvation.

CPy	G° (DMSO)	ΔG° (DMSO)	G° (CH ₂ Cl ₂)	ΔG° (CH ₂ Cl ₂)
1-keto	−877.9177	20.2	−877.9143	17.85
1-enol	−877.9100		−877.9075	

Table 6
Calculated transition energies.

	λ _{max} (nm)	E _T (eV)	f (oscillator strength)	Transition
−H (enol)	289.4	4.27	0.566	71a–72a
−H (keto)	329.4	3.76	0.391	71a–72a
−OCH ₃ (enol)	291.2	4.26	0.593	78a–80a
	277.1	4.47	0.223	79a–80a
−OCH ₃ (keto)	328.2	3.78	0.374	79a–80a
	293.3	4.23	0.369	78a–80a
−NO ₂ (enol)	297.5	4.17	0.506	82a–83a
−NO ₂ (keto)	337.8	3.67	0.351	82a–83a

2.11.2. Electronic spectra

Electronic spectra were calculated for the keto and enol forms of the three compounds using the CAM-B3LYP functional and 6-311 + G(d,p) basis set. The calculated transition energies are consistently higher than those observed experimentally (Table 6). For each compound, the keto form is predicted to absorb at a lower energy than the enol form. The main transition in the 300 nm region of both forms of CPy corresponds to a π–π* transition from the HOMO (71a) to the LUMO (72a) of the compound. Similar transitions are calculated for the tautomers of substituted CPy, but an additional transition from the HOMO-1 to LUMO is also predicted for both keto and enol forms of −OCH₃-CPy. This is consistent with the observation of a second absorption in the spectrum of −OCH₃-CPy (Fig. 5). Isosurfaces of the HOMO-1, HOMO and LUMO of the keto-form of each compound are shown in Fig. 11. The isosurfaces for the frontier orbital of the enol forms are similar.

3. Conclusion

Cyanopyridone (CPy) and its derivatives (−OCH₃ and −NO₂) were synthesized and the solvatochromic behavior was investigated in various solvents. It was found that the spectral shift was sensitive to solvent polarity. The calculated pK_a value for CPy was found to be 9.50 ± 0.57, whereas, for the nitro and methoxy substituted CPy, the values were 8.52 ± 0.36 and 11.04 ± 0.21 respectively. K_{eq} values for keto–enol tautomerism were evaluated for CPy from NMR data and were found to be in agreement with the theoretical calculations. Preferential solvation of CPy in DMSO + CH₂Cl₂ or *i*-PrOH were also studied. An ideal behavior was observed in DMSO + *i*-PrOH mixtures, whereas, in DMSO/CH₂Cl₂ mixture, the solute was more solvated by CH₂Cl₂ in lower mole fractions of DMSO and was preferentially solvated by DMSO beyond 0.3 mol ratio. The calculations using the PCM model indicated ΔG° values favoring the keto form in both dichloromethane and DMSO. The main transition in the 300 nm region of both forms of CPy corresponds to a π–π* transition from the HOMO (71a) to the LUMO (72a) of the compound.

References

- [1] I. Hurjui, L.M. Ivan, D.O. Dorohoi, Spectrochim. Acta A 102 (2013) 219–225.
- [2] Y. Sun, X. Liang, Y. Zhao, J. Fan, Spectrochim. Acta A 102 (2013) 194–199.
- [3] M.S. Zakerhamidi, K. Nejati, Sh.G. Sorkhabi, M. Saati, J. Mol. Liq. 180 (2013) 225–234.
- [4] J.P. Graham, M.A. Rauf, S. Hisaindee, M. Nawaz, J. Mol. Struct. 1040 (2013) 1–8.
- [5] M. Mogren, K. Al-Farhan, Ahmed A. Hasanein, J.Saudi Chem.Soc. 17 (2013) 87–95.
- [6] M.A. Rauf, S. Hisaindee, J. Mol. Struct. 1042 (2013) 45–56.
- [7] M.A. Rauf, J. Graham, S.B. Bukallah, M.A.S. Al-Saedi, Spectrochim. Acta A 72 (2009) 133–137.
- [8] Y.G. Sidir, I. Sidir, Spectrochim. Acta A 102 (2013) 286–296.
- [9] D.Z. Mijin, G.S. Uscumlic, N.U.P. Janjic, N.V. Valentic, Chem. Phys. Lett. 418 (2006) 223–229.
- [10] M.S. Masoud, S.S. Hagagg, A.E. Ali, N.M. Nasr, Spectrochim. Acta A 94 (2012) 256–264.
- [11] R. Menzel, S. Kupfer, R. Mede, H. Görls, L. González, R. Beekert, Tetrahedron 69 (2013) 1489–1498.
- [12] S. Hisaindee, J. Graham, M.A. Rauf, M. Nawaz, J. Mol. Liq. 169 (2012) 48–53.
- [13] L. He, H.S. Freeman, L. Lu, S. Zhang, Dyes Pig. 91 (2011) 389–395.

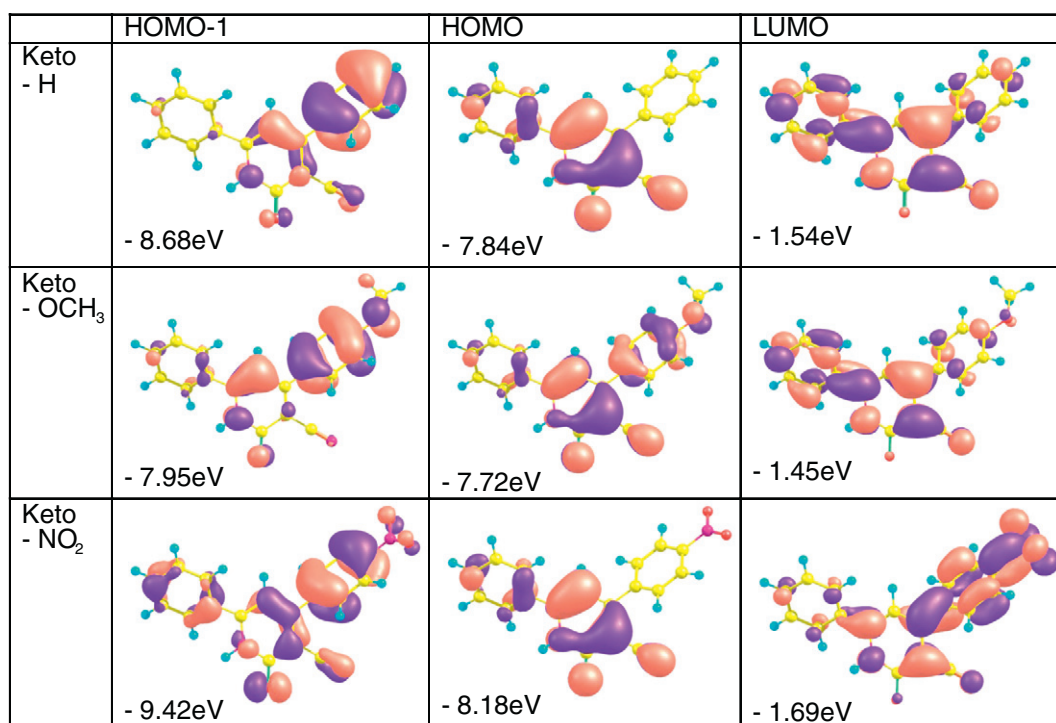


Fig. 11. Orbital isosurfaces of the three compounds.

- [14] Y.L. Sim, N. Omer, M.N. Khan, L.M. Pratt, *Tetrahedron* 69 (2013) 2524–2533.
- [15] Q. Li, L.A. Mitscher, L.L. Shen, *Med. Res. Rev.* 20 (2000) 231–293.
- [16] P.S. Nagle, Y.A. Pawar, A.E. Sonawane, S.M. Bhosale, D.H. More, *Med. Res. Rev.* 12 (2012) 1395–1402.
- [17] A.Z. Michelson, A. Petronico, J.K. Lee, *J. Org. Chem.* 77 (2012) 1623–1631.
- [18] M.J. Frisch, G.W. Trucks, H.B. Schlegel, G.E. Scuseria, M.A. Robb, J.R. Cheeseman, G. Scalmani, V. Barone, B. Mennucci, G.A. Petersson, H. Nakatsuji, M. Caricato, X. Li, H.P. Hratchian, A.F. Izmaylov, J. Bloino, G. Zheng, J.L. Sonnenberg, M. Hada, M. Ehara, K. Toyota, R. Fukuda, J. Hasegawa, M. Ishida, T. Nakajima, Y. Honda, O. Kitao, H. Nakai, T. Vreven, J.A. Montgomery Jr., J.E. Peralta, F. Ogliaro, M. Bearpark, J.J. Heyd, E. Brothers, K.N. Kudin, V.N. Staroverov, R. Kobayashi, J. Normand, K. Raghavachari, A. Rendell, J.C. Burant, S.S. Iyengar, J. Tomasi, M. Cossi, N. Rega, J.M. Millam, M. Klene, J.E. Knox, J.B. Cross, V. Bakken, C. Adamo, J. Jaramillo, R. Gomperts, R.E. Stratmann, O. Yazyev, A.J. Austin, R. Cammi, C. Pomelli, J.W. Ochterski, R.L. Martin, K. Morokuma, V.G. Zakrzewski, G.A. Voth, P. Salvador, J.J. Dannenberg, S. Dapprich, A.D. Daniels, Ö. Farkas, J.B. Foresman, J.V. Ortiz, J. Cioslowski, D.J. Fox, *Gaussian 09, Revision C01*, Gaussian, Inc., Wallingford CT., 2009.
- [19] T. Yanai, D.P. Tew, N.C. Handy, *Chem. Phys. Lett.* 393 (2004) 51–57.
- [20] A.D. Becke, *J. Chem. Phys.* 98 (1993) 5648–5652.
- [21] C. Adamo, V. Barone, *J. Chem. Phys.* 110 (1999) 6158–6162.
- [22] L.C. Zhou, G.J. Zhao, J.F. Liu, K.L. Han, Y.K. Wu, X.J. Peng, M.T. Sun, *J. Photochem. Photobiol. A* 187 (2007) 305–310.
- [23] İ. Sıdır, E. Taşal, Y. Gülseven, T. Güngör, H. Berber, C. Öğretir, *Int. J. Hydrogen Energy* 34 (2009) 5267–5273.
- [24] S.M. Hisaindee, J. Graham, M.A. Rauf, M. Nawaz, *J. Mol. Liq.* 169 (2012) 48–53.
- [25] O.A. Adegoke, *Spectrochim. Acta A* 83 (2011) 504–510.
- [26] J.H. Shi, C.H. Fan, *Spectrochim. Acta A* 95 (2012) 230–234.
- [27] V. Amenta, J.L. Cook, C.A. Hunter, C.M.R. Low, J.G. Vinter, *J. Phys. Chem. B* 116 (2012) 14433–14440.
- [28] A. Maitra, S. Bagchi, *J. Phys. Chem. B* 112 (2008) 9847–9852.
- [29] L.S. Frankel, C.H. Langford, T.R. Stengle, *J. Phys. Chem.* 74 (1970) 1376–1381.
- [30] G. Suganthi, C. Meenakshi, V. Ramakrishnan, *J. Fluoresc.* 20 (2010) 95–103.
- [31] T. Bevilaqua, T.F. Goncalves, C.deG. Venturini, V.G. Machado, *Spectrochim. Acta A* 65 (2006) 535–542.
- [32] C. Reichardt, T. Welton, *Solvents and solvent effects in organic chemistry*, 4th ed. Wiley-VCH, Weinheim, Germany, 2010.